MOLECULAR AND CELLULAR BIOLOGY, Nov. 1983, p. 1889–1897
0270-7306/83/111889-09$02.00/0

Vol. 3, No. 11

Oxalurate Induction of Multiple *URA3* Transcripts in *Saccharomyces cerevisiae*

RICHARD G. BUCKHOLZ AND TERRANCE G. COOPER*
Department of Biological Sciences, University of Pittsburgh, Pittsburgh, Pennsylvania 15260

Received 15 April 1983/Accepted 9 August 1983

The *URA3* gene from *Saccharomyces cerevisiae* is localized on a 1.1-kilobase (kb) DNA fragment. By using this fragment as a hybridization probe, we found that oxalurate, a gratuitous inducer of the allantoin degradative system, also serves to induce *URA3* specific RNA. This response is restricted to oxalurate; other conditions which bring about high-level synthesis of the allantoin degradative enzymes did not produce the effect. Two classes of RNA (1.0 and 1.5 kb) were found to be oxalurate induced. Both classes are encoded by the *URA3* gene, overlap, and probably do not significantly differ at their 5′ termini. Northern blot mapping of the transcripts indicated that the 1.5-kb transcript was likely encoded by sequences extending up to 0.5 kb downstream from the 3′ terminus of the 1.0-kb transcript. Analysis of the endpoints of the major 1.0-kb *URA3* transcript by S1 nuclease mapping revealed the existence of two 5′ termini, separated by 5 to 10 nucleotides, and seven 3′ termini, separated by 5 to 20 nucleotides each, over a range of about 70 bases.

In *Saccharomyces cerevisiae*, the biosynthesis of uracil requires the products of at least five unlinked genes, *URA1* to *URA5*. Lacroute has proposed a regulatory system in which the last enzyme of the pathway, orotidine-5′-phosphate decarboxylase (the *URA3* gene product), is induced by dihydroorotate (12). Bach et al. (1) reported that the level of *URA3* mRNA, as measured by hybridization to *URA3* DNA, varies coordinately with the enzyme activity. From this they concluded that the *URA3* gene was transcriptionally regulated. Plasmids carrying the *URA3* gene on a 1.1-kilobase (kb) DNA insert have been frequently used as yeast cloning vectors. However, exploitation of this system as a model of gene expression has been somewhat hindered by the modest levels of *URA3* mRNA found in the cell and by the limited degree of *URA3* gene induction. One problem in this respect is that most, if not all, wild-type cells are impermeable to dihydroorotate, the presumed inducer of *URA3* gene expression (12). Therefore, one must either bring about induction indirectly or use a specific mutant construction which will accumulate exogenously provided dihydroorotate (12).

In studies of the allantoin degradative system (18), we have used the compound oxalurate as a nonmetabolizable analog of allophanic acid, the native pathway inducer (5). We report here that oxalurate also brings about an increase in the level of *URA3*-specific mRNA and that this effect is separate from control of the allantoin pathway. Further, we provide evidence that transcription of the *URA3* gene results in production of multiple, discrete, polyadenylated [poly(A)$^+$] RNA species.

MATERIALS AND METHODS

Strains, plasmids, and growth conditions. All of the strains used in this work are listed in Table 1. Plasmid pFL1, derived from a yeast chromosomal bank provided by F. Lacroute, is composed of plasmid pBR322 DNA, a 1.1-kb *Hin*dIII fragment of yeast chromosomal DNA containing the *URA3* gene, and the *Eco*RI D fragment of the yeast 2u plasmid (3). Plasmid yIP5, a gift from R. Davis, is composed of a 1.1-kb *Hin*dIII fragment containing *URA3* inserted by deoxyguanine-deoxycytidine tailing into the unique *Ava*I site of pBR322 (17). Plasmid pBRD was a gift from Tom Petes and is composed of a 0.66-kb yeast chromosomal fragment containing portions of the 5.8S and 18S ribosomal RNA genes inserted into the unique *Eco*RI site of plasmid pBR322.

Growth conditions and media for preparation of RNA from yeast strains and for preparation of plasmids from *Escherichia coli* were as previously described (19). Proline (0.1% [wt/vol]) was utilized as the sole source of nitrogen unless otherwise stated.

Preparation of RNA and radioactive DNA restriction fragments. Extraction of RNA from yeast cells grown on Wickerham medium (22) was essentially as described by Carlson and Botstein (2). RNA prepared in this manner was enriched for poly(A)$^+$ RNA by two passages over an oligodeoxythymidylate cellulose column as described earlier (19). Procedures for Northern blot hybridization were also described earlier (19).

Restriction enzyme digestion, 5′-end labeling of DNA fragments, and elution of radioactive fragments

TABLE 1. Strains used in this work

S. cerevisiae strain	Genotype
M970	MATα *lys2* / MATa *lys5*
M1081	MATα *lys2 dal80-1* / MATa *lys5 dal80-1*
M1407	MATα *lys5 dal81-2* / MATa *lys2 dal81-2*

from 5% acrylamide gels were performed by the procedures of Maxam and Gilbert (14). The 3'-end labeling of DNA restriction fragments was as described by Maniatis et al. (13). Strand separation of end-labeled DNA fragments was performed either in 1.75% agarose gels prepared in 1× TAE buffer (19) for fragments above 1.0 kb or in 5% low bis-acrylamide gels, both as described by Maniatis et al. (13). All enzymes were purchased from New England Bio-Labs or Bethesda Research Laboratories.

S1 nuclease mapping of 3' and 5' RNA termini. S1 nuclease mapping protocols and solutions were based on those reported by Favaloro et al. (7). The 3'- or 5'-end-labeled fragment was coprecipitated with 20 μg of the appropriate poly(A)$^+$ RNA preparation and 100 μg of *E. coli* tRNA (Sigma Chemical Co.). The precipitate was redissolved in 1× hybridization buffer (prepared by mixing 4 volumes of deionized formamide with 1 volume of a concentrated solution composed of 2 M NaCl, 5 mM EDTA, and 0.2 M PIPES [piperazine-*N*,*N*'-bis-2-ethanesulfonic acid] [pH 6.4]) and incubated at 44°C for 3 h. Hybridization was terminated by addition of 300 μl ice-cold nuclease S1 digestion buffer (0.28 M NaCl, 4.5 mM $ZnSO_4$, 50 mM sodium acetate [pH 4.6], 20 μg of denatured salmon sperm DNA per ml, 130 to 400 U of nuclease S1 per ml). The digestion mixture was incubated for 30 min at 37°C unless otherwise stated. Digestion was terminated by addition of 30 μl of ice-cold termination mix (4.0 M ammonium acetate, 0.1 M EDTA, 200 μg of *E. coli* tRNA per ml) followed by ethanol precipitation. The precipitate was redissolved in 5 μl of 0.1 M NaOH–5 mM EDTA and 5 μl of a urea-dye mixture (32% urea, 0.1% bromophenol blue, 0.1% xylene cyanol [wt/vol]) was added, followed by heating at 90°C for 2 min. The sample was rapidly chilled on ice and loaded onto a 8.3 M urea–6% acrylamide gel (15 by 20 cm). Electrophoresis was carried out for 10 to 12 h at 8 V/cm. Size standards were pBR322 digested with *Ava*II-*Hin*dIII and 3'-end labeled with the Klenow fragment of DNA polymerase.

RESULTS

Oxalurate-mediated induction of two RNA species complementary to yIP5 DNA. While studying oxalurate-mediated induction of the allantoin pathway genes, we observed two additional RNA species (1.0 and 1.5 kb) responding to the presence of this gratuitous inducer. These species were present at high levels when oxalurate was provided in the growth medium and at markedly low levels when it was not (Fig. 1, lanes A and B). Both RNA species were found to be complementary to the 1.1-kb insert of vector yIP5, a DNA fragment which has been shown by others to carry the *URA3* gene (1, 3). As shown in Fig. 1, high levels of hybridization were observed when plasmid yIP5 was used as a probe, yet no hybrid formation could be detected when plasmid pBR322 was used instead (lane C). These two plasmids differ only by the 1.1-kb *URA3* insert, which is contained in the former.

The response of these RNA species to the gratuitous inducer of the allantoin degradative enzymes prompted us to ascertain whether their production was also influenced by the allantoin

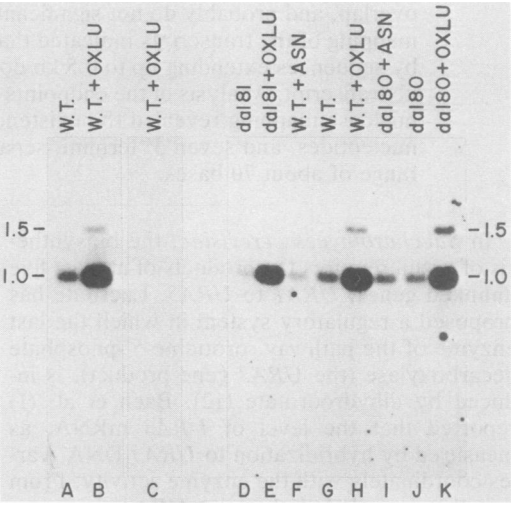

FIG. 1. Northern blot analysis of poly(A)$^+$ RNA derived from wild-type (WT) and mutant strains of *S. cerevisiae* grown in the presence or absence of oxalurate (OXLU). Five micrograms of each poly(A)$^+$ RNA preparation were separated on formaldehyde agarose gels, transferred to nitrocellulose, and hybridized to the indicated probe as described in the text. Poly(A)$^+$ RNAs prepared from M970 cultured in the absence (lane A) and presence (lanes B and C) of OXLU were probed with nick-translated yIP5 DNA (lanes A and B) or pBR322 DNA (lane C). Poly(A)$^+$ RNAs isolated from strain M1045 (*dal81/dal81*, lanes D to E), strain M970 (WT, lanes F to H), and strain M1081 (*dal80/dal80*, lanes I to K) cultured in the absence (lanes D, G, and J) or presence (lanes E, H, and K) of OXLU were probed with nick-translated yIP5 DNA. Lanes F and I contain poly(A)$^+$ RNAs isolated from strains cultured with 0.1% (wt/vol) asparagine (ASN) as the sole nitrogen source. RNA sizes are in kilobases. The size standards we used were derived from pBR322 DNA digested with *Ava*II or *Alu*I, heated at 90°C for 15 min, and separated in the same fashion as for the RNAs. The fragments used for calibration were 1.7, 1.4, and 0.3 kb (*Ava*II digest) and 0.9, 0.7, 0.5, and 0.4 kb (*Alu*I digest).

pathway regulatory elements. To accomplish this, we determined the amounts of the two species in wild-type and *dal80* and *dal81* mutant strains. Mutation of the *DAL80* locus has been shown to result in constitutive expression of the allantoin pathway genes (4). *Dal81* mutants, on the other hand, have pleiotropically lost the ability to induce the expression of these genes (21). As shown in Fig. 1, lanes D to K, neither mutation affected production of the two RNA species. On the contrary, the mutant and wild-type strains behaved identically; only the presence of oxalurate in the culture medium significantly affected the transcript levels. Furthermore, growth of wild-type strain M970, with urea as the sole nitrogen source, and growth of a *dur2* mutant strain in minimal proline medium did not result in an increase of the transcripts hybridizing to yIP5 DNA (data not shown). High levels of the allantoin degradative enzymes are produced in both of these situations (5). These experiments ruled out the possibility that oxalurate-mediated increases in *URA3* gene expression were related to the allantoin degradative system. The observed induction of poly(A)$^+$ *URA3* mRNA was specifically dependent on the presence of oxalurate.

The 1.0-kb and 1.5-kb species are discrete transcripts. The observation that apparently two distinct transcripts were induced by oxalurate was puzzling. Since the larger 1.5-kb transcript migrated just in front of the 1.7-kb 18S rRNA, it was possible that 18S rRNA contamination of the enriched poly(A)$^+$ RNA resulted in the artifactual appearance of a species migrating at approximately 1.5 to 1.7 kb. Such an artifact would have conceivably resulted from concentration of *URA3* mRNA that "tailed" behind the main 1.0-kb band; such tailing is often observed in overloaded formaldehyde gels. The 18S rRNA would serve in a snow plow-like fashion according to this hypothesis. To determine whether this was the case, we conducted the following experiment. Two circular wells were cut near one corner of a large 1.5% agarose formaldehyde gel. Ten micrograms of poly(A)$^+$ RNA isolated from an oxalurate-induced culture was loaded into each well and electrophoretically fractionated. The outside lane was then cut off and set aside, and the remainder of the gel was rotated 90° and subjected to electrophoresis in the second dimension. After the outer lane was reassembled with the rest of the gel, the entire contents were transferred to nitrocellulose. The resulting Northern blot was hybridized to radioactive yIP5 DNA, and the hybrids were visualized by autoradiography. The same filter was then hybridized a second time to radioactive pBRD, a pBR322 derivative containing portions of the yeast 18S and 5.8S rRNA genes. If the 1.5-kb species was an artifact caused by a snow plow effect of contaminating 18S rRNA, then the first-dimension 1.5-kb spot would be predicted to migrate either as a smear or as a 1.0-kb species in the second dimension. This result was expected because the 18S rRNA would not migrate behind the 1.5-kb species in the second dimension, but rather would be adjacent and parallel to it. As shown in Fig. 2, the 1.5-kb transcript clearly separated from the 18S rRNA and continued to migrate as a discrete species in the second dimension. The 5.8S rRNA migrated to a position near the bottom of the gel. The spot appearing directly below the 1.0-kb transcript was likely due to RNA degradation; it appeared in this preparation of poly(A)$^+$ RNA, but was absent from others. This experiment indicated that the 1.5-kb and 1.0-kb RNAs were discrete oxalurate-inducible transcripts homologous to the 1.1-kb *Hin*dIII fragment carried by yIP5.

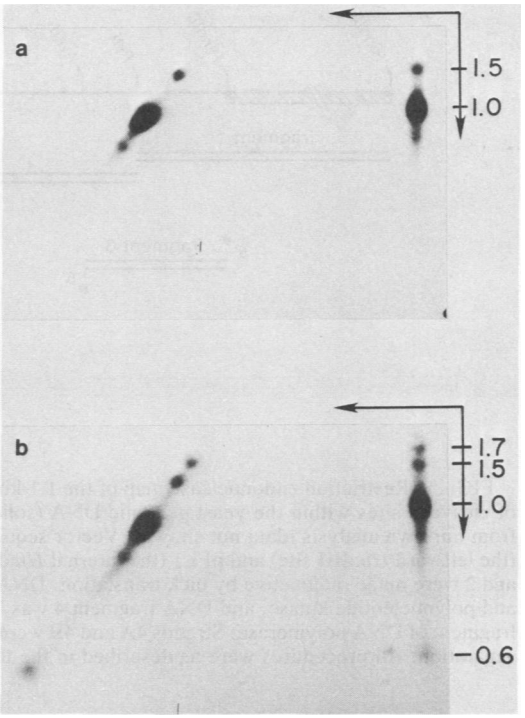

FIG. 2. Hybridization analysis of poly(A)$^+$ RNAs derived from strain M970 cultured in the presence of oxalurate. (a) Poly(A)$^+$ RNA was fractionated in two dimensions (arrows), transferred to nitrocellulose paper, and hybridized with plasmid yIP5 DNA which had been made radioactive by nick translation. (b) Same filter as above was hybridized a second time with plasmid pBRD DNA which had been made radioactive by nick translation. The positions of the *URA3* and rRNA transcripts are indicated. RNA sizes are indicated in kilobases.

Mapping the *URA3* transcripts. The two coordinately induced transcripts could have been

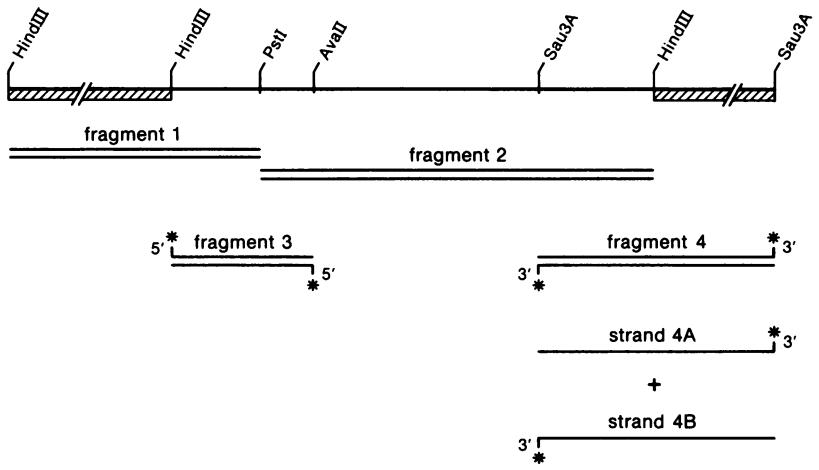

FIG. 3. Restriction endonuclease map of the 1.1-kb DNA fragment containing the *URA3* gene. The locations of cleavage sites within the yeast genomic DNA (solid lines) were derived from the published maps (1, 3) and from our own analysis (data not shown). Vector sequences represent a composite of the sites in plasmids yIP5 (the leftward *Hin*dIII site) and pFL1 (the internal *Hin*dIII sites and the rightward *Sau*3A site). DNA fragments 1 and 2 were made radioactive by nick translation. DNA fragment 3 was labeled at the 5′ termini with [α-^{32}P]ATP and polynucleotide kinase, and DNA fragment 4 was labeled at the 3′termini with [α-^{32}P]dCTP and the Klenow fragment of DNA polymerase. Strands 4A and 4B were prepared from DNA fragment 4 by electrophoretic strand separation. All procedures were as described in the text.

transcribed in several different ways: (i) with opposite polarities (head-to-head or tail-to-tail), (ii) with the same polarity, but in a nonoverlapping manner (head-to-tail), or (iii) overlapping at the 5′ or 3′ termini. Figure 3 details the structure of the 1.1-kb *Hin*dIII DNA fragment inserted into plasmids yIP5 and pFL1, and the DNA fragments used to analyze transcription of the *URA3* gene. Our initial experiment to distinguish among the above situations involved determining whether the 1.0- and 1.5-kb mRNAs were transcribed with the same polarity. To accomplish this, the 1.1-kb *Hin*dIII fragment from plasmid pFL1 was isolated, 5′-end labeled, and subjected to electrophoretic strand separation. The separated strands of DNA were then used to probe poly(A)$^+$ RNA isolated from oxalurate-induced cells. As shown in Fig. 4, only the slowly migrating strand (lane B) hybridized to the separated RNA species. We concluded from this that both RNAs were encoded by the same DNA strand.

Since this result ruled out the possibility of head-to-head or tail-to-tail transcription, we next set out to locate the 1.0- and 1.5-kb transcripts within the 1.1-kb DNA fragment. We argued that the 1.0-kb mRNA species was probably encoded entirely within the 1.1-kb *Hin*dIII fragment, because it had already been shown to be sufficient for complementation of *ura3* mutations (3). The 1.5-kb transcript, on the other hand, was longer than the 1.1-kb insert in plasmid yIP5. Therefore, one or both of its termini must be outside of this region. To more closely map these transcripts, we probed induced poly(A)$^+$ RNAs with DNA fragments representing the leftward *Pst*I-*Hin*dIII region (Fig. 3, fragment 1) and the rightward *Pst*I-*Hin*dIII region (fragment 2) of the 1.1-kb insert. Only fragment 2 hybridized strongly to the two transcripts (Fig. 4, lane D). Fragment 1 hybridized very weakly, if at all. Extremely long exposures (7 to 14 days) of the autoradiogram revealed barely detectable hybridization with the 1.0-kb transcript. This was consistent with the conclusion that one end of the small transcript was situated either near or just to the left of the *Pst*I site, located 0.20 kb from the left end of the insert. A similar experiment was carried out by using the small *Hin*dIII-*Ava*II fragment (fragment 3) as a probe. As shown in Fig. 4, lane E, this fragment hybridized to both transcripts. This result localized the terminus of the larger transcript to the 0.175-kb region between the *Pst*I and *Ava*II sites. We have not excluded, however, the possibility that it is situated just to the left of the *Pst*I site. Since fragment 2 was only about 1.0 kb long, which is the approximate length of the smaller mRNA, these results and the coordinate induction behavior suggested a model in which the two transcripts were heavily overlapped, possibly beginning at a common 5′ end. Further, the 1.5-kb transcript was likely encoded by genomic sequences extending up to 0.5 kb beyond the right-hand *Hin*dIII site of the insert.

We began testing this hypothesis by using S1 nuclease mapping to locate the 5′ and 3′ termini of the *URA3* transcripts. To accomplish this, the 5′ termini of the 0.38-kb *Ava*II-*Hin*dIII fragment (Fig. 3, fragment 3) were labeled with polynucleotide kinase, and the 3′ termini of the 0.57-kb *Sau*3A fragment (fragment 4) were labeled with the Klenow fragment of DNA polymerase I. The labeled fragments were hybridized to poly(A)$^+$ RNA isolated from oxalurate-induced cells. The unhybridized, single-stranded nucleic acids were then digested with S1 nuclease; the remaining duplexes were denatured, and the fragments were resolved on a 6% urea-polyacrylamide gel. As shown in Fig. 4, lane H, two distinct fragments of about 0.193 and 0.200 kb were protected from S1 nuclease attack when poly(A)$^+$ RNA was present. There was no protection of the probe when poly(A)$^+$ RNA was omitted from the initial hybridization mixture (Fig. 4, lane G). The fact that the two protected fragments were found to be of the same intensity is consistent with the suggestion that the 1.0-kb and 1.5-kb oxalurate-inducible *URA3* transcripts begin at two common sites. We must emphasize, however, that a situation in which the 1.5-kb transcript protected one of these sites while the 1.0-kb transcript protected both of them would go undetected.

Protection of the 3′-labeled DNA fragment by poly(A)$^+$ RNA gave a quite different result. Instead of producing two protected fragments corresponding to the 1.0-kb and 1.5-kb transcripts, there were fully seven discrete fragments, ranging from about 0.190 to 0.260 kb (Fig. 5, lane I). The longest fragment (260 nucleotides) represented protection of the entire *Sau*3A-*Hin*dIII probe. This is the expected nuclease S1 digestion product of a hybrid formed between the sense strand of fragment 4 and the 1.5-kb transcript. Two other fragments of 190 and 220 nucleotides were present as major species, whereas four minor species of 210, 230, 240, and 255 nucleotides were also obtained. Such a range of putatively protected fragments could be interpreted as an artifact caused by the conditions of the nuclease S1 protection experiment, rather than representative of the locations of multiple poly(A) sites. Again, protection was entirely dependent on the presence of poly(A)$^+$ RNA (Fig. 5, lanes E, F, H, and I). To ensure that stabilization of the DNA duplex did not produce an artifactual array of nuclease S1 digestion fragments, the strands of fragment 4, labeled at their 3′ termini, were separated and used individually to map the 3′ mRNA termini (Fig. 5, lanes A to F). When the faster migrating, anti-sense strand was used, no protected fragments were observed (lane C). The slowly migrating, sense strand (lane F), on the other hand,

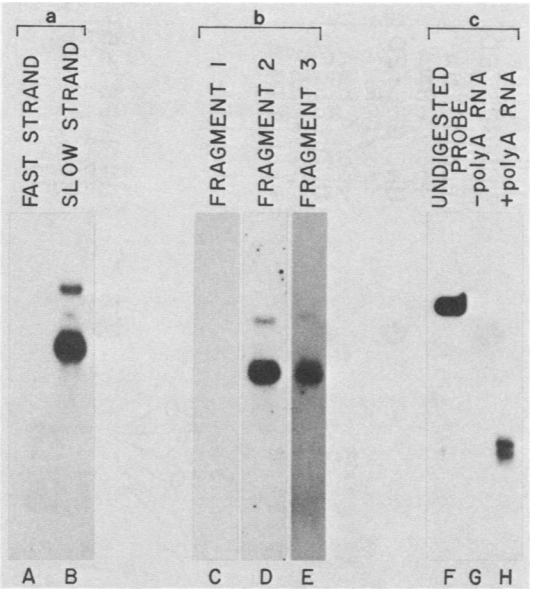

FIG. 4. (a) Northern blot analysis of the polarity of the *URA3* RNA transcripts. Poly(A)$^+$ RNA derived from strain M970 cultured in the presence of oxalurate was separated on formaldehyde agarose gels and transferred to nitrocellulose paper. The filter was separated into strips, and the individual strips were hybridized with the designated 5′-end-labeled strand of the 1.1-kb *Hin*dIII fragment. (b) Location of the leftward termini of the *URA3* transcripts. Induced RNA was fractionated and transferred to strips of nitrocellulose paper as described above, and the individual strips were hybridized with the designated DNA fragment from Fig. 3. The filters in lanes C and D were hybridized with nick-translated fragments, and the filter in lane E was hybridized with the 5′-end-labeled fragment. (c) S1 nuclease mapping of the 5′ termini of the *URA3* transcripts. A total of 30,000 cpm of the *Ava*II-*Hin*dIII fragment (DNA fragment 3; Fig. 3) which had been 5′-end-labeled with [α-^{32}P]ATP and polynucleotide kinase was hybridized with poly(A)$^+$ RNA (1 mg/ml) derived from an induced culture of strain M970 as described in the text and digested with 200 U of nuclease S1 per ml. The protected DNA sequences were fractionated through a 6% polyacrylamide gel under denaturing conditions and detected by autoradiography. Lanes: F, undigested DNA fragment 3; G, control hybridization with no poly(A)$^+$ RNA; H, 1 mg of M970 poly(A)$^+$ RNA per ml. Fragment sizes were determined by comparison with 3′-end-labeled *Ava*II-*Hin*dIII digestion products of pBR322. The sizes of the fragments were derived from published pBR322 sequence data (20) and were 1,743, 769, 664, 303, 279, 249, 222, 88, and 42 nucleotides, respectively.

produced an array of S1-resistant fragments identical to that seen when the double-stranded probe was used. This rules out DNA duplex formation as a factor in the production of the S1 digestion fragments.

Multiple S1-resistant fragments can also arise

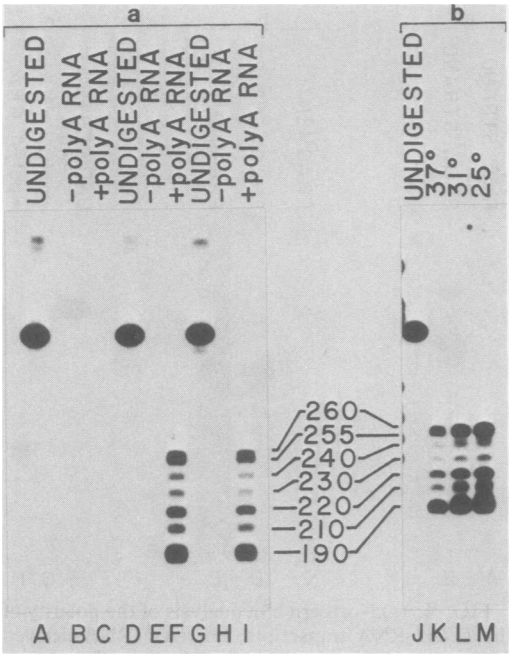

FIG. 5. S1 nuclease mapping of the 3′ termini of the *URA3* transcripts. The *Sau*3A fragment (DNA fragment 4; Fig. 3) or its individual strands which had been labeled at the 3′ end with [α-^{32}P]dCTP and Klenow DNA polymerase were hybridized with poly(A)$^+$ RNA, digested with nuclease S1, separated, and processed as described in the legend to Fig. 4. (a) Lane A contains undigested strand 4A, lane D contains undigested DNA strand 4B, and lane G contains undigested fragment 4. Lanes B, E, and H contain control hybridization reactions devoid of poly(A)$^+$ RNA. Lanes C, F, and I contained 1 mg of poly(A)$^+$ RNA per ml. (b) Effects of varying the temperature of nuclease S1 digestion on nuclease S1 products of induced M970 poly(A)$^+$ RNA-strand 4B DNA hybrids. Poly(A)$^+$ RNA concentration was 0.5 mg/ml; all other conditions were the same as those above for lane F, except that S1 digestion was carried out at 37°C (lane K), 31°C (lane L), or 25°C (lane M) as indicated.

from nonuniform trimming of ragged DNA overhangs, which are in turn dependent on the severity of the S1 digestion conditions used (11). In this case, however, heterogeneity is on the order of one to five nucleotides (9), which is below the resolution of the gels in Fig. 5. At any rate, varying the S1 concentration over a threefold range affected neither the size nor relative intensities of the S1 protection fragments (data not shown). A third source of heterogeneity such as that shown in Fig. 5 is nonrandom digestion of the DNA-RNA hybrid under conditions favoring selective breathing at various points within the hybrid; the problem is intensified by the AT-rich sequences usually found in 3′ flanking regions of yeast genes (23). This possibility was examined by reducing the temperature of S1 digestion, which should increase the stability of AT base pairing and thereby decrease selective "breathing" of the hybrid (8, 10). As shown in Fig. 5, lanes J to M, decreasing the temperature during S1 digestion did not alter the sizes or relative intensities of the S1-resistant fragments. The increase in intensity of each band as the temperature was lowered resulted from a decrease in the specific activity of the S1 nuclease at the lower temperature. The lack of evidence for breathing or S1 end nibbling led us to conclude that each of the fragments observed in lanes F and I of Fig. 5 might well represent the 3′ terminus of a discrete *URA3* mRNA transcript.

DISCUSSION

The availability of nonmetabolizable inducer analogs has greatly facilitated the investigation of gene regulation. In particular, oxalurate has been very useful during our past studies of the allantoin degradative system wherein it induces expression of these genes as efficiently as the native inducer, allophanate (5). Until now, we felt that its action was exclusively restricted to the allantoin system. However, the data presented in this report clearly demonstrate that oxalurate can also serve as an equally efficient inducer of the *URA3* gene. This ability likely derives from the structural similarity that exists between oxalurate and the suggested native inducer of this gene, dihydroorotate (Fig. 6) (12). In spite of the fact that oxalurate can serve as inducer for both systems, two observations point to the physiological individuality of uracil biosynthesis and allantoin degradation in vivo. First, *URA3* gene expression was not induced by provision of urea as a nitrogen source, a physiological condition which results in induction of the allantoin system. Second, production of *URA3* transcripts was immune to the effects of mutation of either of the allantoin system regulatory genes.

The ability of oxalurate to serve as a gratuitous inducer of both the allantoin system and *URA3* gene raises an interesting question: why does allophanate fail to induce expression of *URA3*? Conversely, is dihydroorotate able to induce expression of the allantoin system genes? Comparison of the three structures in Fig. 6 may provide some insight into this paradox, though the correlations derived are not easily tested in a direct manner. Allophanate is missing the carboxyl group which extends from the six-membered rings of both dihydroorotate and oxalurate. If this group was important for either binding of the inducer to its cognate control element(s) or subsequent conformational change of that element(s), allophanate would probably

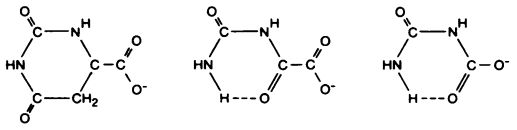

FIG. 6. Structures of the *URA3* gene native inducer dihydroorotate, the allantoin system native inducer allophanate, and the gratuitous analog oxalurate.

fail to effectively substitute for dihydroorotate. If, conversely, the C-1 oxygen of allophanate functioned similarly in control of the allantoin system genes, dihydroorotate would unlikely be able to fill this role due to the presence of a methylene group in this position. According to this explanation, oxalurate functions well for both systems because it possesses the structural requirements of each. It is conceptually feasible to test directly whether or not dihydroorotate will serve as an inducer of the allantoin degradative system by using the mutant cited earlier. Since we do not have this mutant at present, the experiment has not yet been performed.

Increased *URA3* gene expression resulting from induction with oxalurate made it possible for us to recognize the existence of two major *URA3* transcripts. A 1.0-kb species accounted for about 92% of the total *URA3* homologous RNA, whereas a 1.5-kb transcript accounted for the remaining 8%. Nuclease S1 mapping of the *URA3* 5′ terminus demonstrated the existence of two protected species which differed by only 7 to 10 base pairs (Fig. 4, lane H). The equal amounts of these two species lead us to conclude that the 1.0-kb transcript was composed of species that were represented more or less equally among the two protection fragments. The distribution of 1.5-kb mRNA 5′ termini between the two protection fragments could not be determined from the unfractionated RNA we used. However, hybridization patterns of 1.5-kb RNA species argue that the 5′-terminus of this species is not located in a significantly different region from that observed for the 1.0-kb species and may, in fact, be at the same point. The important point is that the 500-nucleotide difference between the two *URA3* transcripts did not derive from the longer species beginning 0.5 kb upstream from the start site of the 1.0-kb species.

Nuclease S1 mapping of the 3′ termini, on the other hand, revealed seven discrete classes of 3′-terminal protection fragments, each differing in length by about 10 nucleotides (Fig. 7). The 190-nucleotide fragment is by far the most dominant. Next in abundance are the 220- and 255-nucleotide species, followed by those of 260 and 210 nucleotides, respectively. The 230- and 240-nucleotide species were least abundant. The largest protected fragment was of a size expected if the RNA-DNA hybrid extended to the right end of the *URA3* insert. We therefore presume that the 1.5-kb transcript is homologous to genetic material extending beyond what has been cloned in plasmid yIP5. Unavailability of these

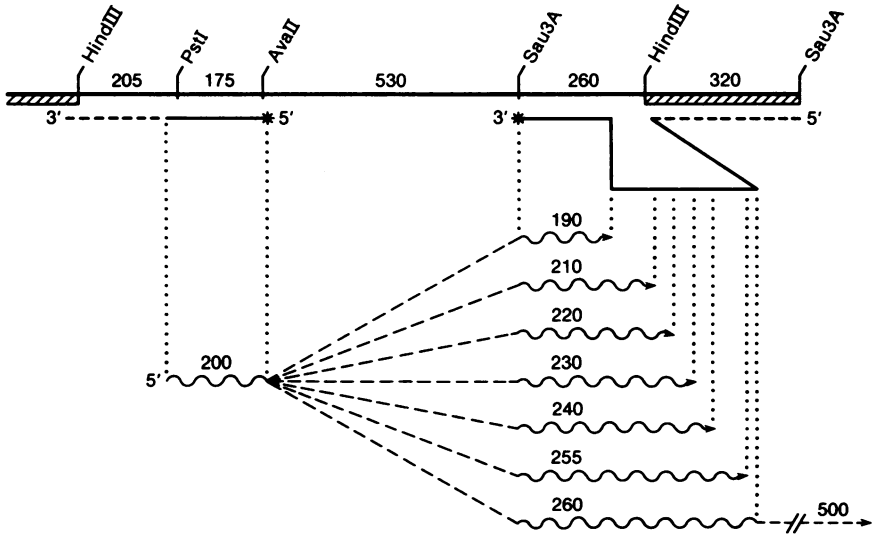

FIG. 7. Alignment of the *URA3* transcripts and the *URA3* gene restriction map. Distances are in nucleotides. Yeast genomic sequences are represented by a solid line, whereas vector sequences are cross-hatched. Lengths of *URA3* RNA fragments (wavy lines) were taken from Fig. 4, lane G, and from Fig. 5. The region between 0.190 kb to the right of the internal *Sau*3A site and the rightward *Hin*dIII site has been expanded for purposes of clarity.

3′ flanking sequences prohibited us from determining whether the 1.5-kb RNA consists of species with heterogeneous ends. It is quite probable that the three smallest protection fragments are generated from termination or processing sites within the 3′ *URA3* sequence published by Zaret and Sherman (23). The major 190-nucleotide fragment, for example, ends in the vicinity of the adenine- and thymine-rich sequence TATATCA, which, interestingly, is before any of the consensus sequences proposed by Zaret and Sherman to be associated with termination or polyadenylation. In a similar manner, all of the remaining fragments, with exception of the 210- and 260-nucleotide species, appear to end in proximity to stretches of adenines and thymines.

We have considered the real possibility of these multiple protection fragments being generated artifactually. Repeated and varied attempts to alter the observed pattern of fragments by changes in the hybridization or S1 digestion conditions were to no avail. This argues positively, but does not prove, that the observed heterogeneity in the 1.0-kb transcripts is real.

From our data, it is not possible to decide whether the heterogeneous 1.0-kb species derive from multiple RNA termination sites followed by polyadenylation of the transcripts produced or, alternatively, multiple processing and polyadenylation of a single long precursor transcript. The same uncertainty surrounds the relationship of the 1.5-kb and 1.0-kb transcripts to one another. It is unclear whether this heterogeneity extends over the 0.5-kb region between the 3′ termini of the 1.0- and 1.5-kb species. However, results from the Northern blots shown in Fig. 1 argue against it. The very wide band observed for the 1.0-kb species is consistent with the heterogeneity we observe. Similar behavior was not observed for the 1.5-kb species or the region of the blot between the 1.0- and 1.5-kb transcripts.

Minor heterogeneity over a 0.06-kb region was observed for the *his4* transcript (6). However, the 3′-S1 map was not presented in that report, making detailed comparison difficult. Four major 3′ termini were reported for the mature *ADR2* mRNA (16). However, the shortest and longest species differed by only four nucleotides, clearly a different situation than that which we observe for *URA3*. Greater formal similarity was observed for the chicken vimentin gene (24). Here, two major transcripts differing in length by 0.250 kb were found. Preliminary data also suggested heterogeneity of the two major species as well. In a similar manner, Parnes et al. reported the occurrence of β_2-microglobulin transcripts which differed in length by over 200 nucleotides (15). Here, as before, heterogeneity was observed at the 3′ termini of the shorter transcripts. In this case, however, the major size classes were correlated with the presence of the hexanucleotide sequence AATAAA hypothesized to play an important signaling role in mammalian cells. It remains to be shown whether analogous signals can be found in flanking sequences of the yeast *URA3* gene.

ACKNOWLEDGMENTS

We thank Francois Lacroute, who provided the yeast chromosomal bank from which plasmid pFL1 was derived. We also appreciate the generous gifts of plasmid yIP5 from Ronald Davis and plasmid pBRD from Tom Petes via John Woolford.

This work was supported by Public Health Service grants GM-19386, GM-20693, and GM-24383 from the National Institute of General Medical Sciences.

LITERATURE CITED

1. **Bach, M. L., F. Lacroute, and D. Botstein.** 1979. Evidence for transcriptional regulation of orotidine-5′-phosphate decarboxylase in yeast by hybridization of mRNA to the yeast structural gene cloned in *E. coli*. Proc. Natl. Acad. Sci. U.S.A. **76**:386–390.
2. **Carlson, M., and D. Botstein.** 1982. Two differentially regulated mRNAs with different 5′ ends encode secreted and intracellular forms of yeast invertase. Cell **28**:145–154.
3. **Chevallier, R., J. Bloch, and F. Lacroute.** 1980. Transcriptional and translational expression of a chimeric bacterial-yeast plasmid in yeasts. Gene **11**:11–19.
4. **Chisholm, G., and T. G. Cooper.** 1982. Isolation and characterization of mutants that produce the allantoin-degrading enzymes constitutively in *Saccharomyces cerevisiae*. Mol. Cell. Biol. **2**:1088–1095.
5. **Cooper, T. G., and R. P. Lawther.** 1973. Induction of the allantoin degradative enzymes in *Saccharomyces cerevisiae* by the last intermediate of the pathway. Proc. Natl. Acad. Sci. U.S.A. **70**:2340–2344.
6. **Donahue, T. F., P. J. Farabaugh, and G. R. Fink.** 1982. The nucleotide sequence of the *HIS4* region of yeast. Gene. **18**:47–59.
7. **Favaloro, J., R. Treisman, and R. Kramer.** 1980. Transcription maps of polyoma virus-specific RNA: analysis by two-dimensional nuclease S1 mapping. Methods Enzymol. **65**:718–749.
8. **Gregory, S. P., N. O. Dillon, and P. H. W. Butterworth.** 1982. The localization of the 5′-termini of *in vivo* and *in vitro* transcripts of a cloned rainbow trout protamine gene. Nucleic Acids Res. **10**:7581–7592.
9. **Grosschedl, R., and M. L. Birnstiel.** 1980. Identification of regulatory sequences in the prelude sequences of an H2A histone gene by the study of specific deletion mutants *in vivo*. Proc. Natl. Acad. Sci. U.S.A. **77**:1432.
10. **Grosveld, G. C., E. de Boer, C. K. Sewmaker, and R. A. Flavell.** 1982. DNA sequences necessary for transcription of the rabbit β-globin gene *in vivo*. Nature (London) **295**:120–126.
11. **Heutschel, C., J. Irminger, P. Bucher, and M. L. Birnstiel.** 1980. Sea urchin histone mRNA termini are located in gene regions downstream from putative regulatory sequences. Nature (London) **285**:147–151.
12. **Lacroute, F.** 1968. Regulation of pyrimidine biosynthesis in *Saccharomyces cerevisiae*. J. Bacteriol. **95**:824–832.
13. **Maniatis, T., E. F. Frisch, and J. Sambrook.** 1982. Molecular cloning, a laboratory manual. Cold Spring Harbor Laboratory, Cold Spring Harbor, N.Y.
14. **Maxam, A. M., and W. Gilbert.** 1980. Sequencing end-labeled DNA with base-specific chemical cleavages. Methods Enzymol. **65**:499–560.

15. **Parnes, J. R., R. R. Robinson, and J. G. Seidman.** 1983. Multiple mRNA species with distinct 3' termini are transcribed from the β_2-microglobulin gene. Nature (London) **302**:449–452.
16. **Russell, D. W., M. Smith, V. M. Williamson, and E. T. Young.** 1983. Nucleotide sequence of the yeast alcohol dehydrogenase II gene. J. Biol. Chem. **258**:2674–2682.
17. **Struhl, K., D. T. Stinchcomb, S. Scherer, and R. W. Davis.** 1979. High frequency transformation of yeast: autonomous replication of hybrid DNA molecules. Proc. Natl. Acad. Sci. U.S.A. **76**:1035–1039.
18. **Sumrada, R., and T. G. Cooper.** 1974. Oxaluric acid: a non-metabolizable inducer of the allantoin degradative enzymes in *Saccharomyces cerevisiae*. J. Bacteriol. **117**:1240–1247.
19. **Sumrada, R. A., and T. G. Cooper.** 1982. Isolation of the *CAR1* gene from *Saccharomyces cerevisiae* and analysis of its expression. Mol. Cell. Biol. **2**:1514–1523.
20. **Sutcliffe, J. G.** 1978. Complete nucleotide sequence of the *Escherichia coli* plasmid pBR322. Cold Spring Harbor Symp. Quant. Biol. **43**:77–90.
21. **Turoscy, V., and T. G. Cooper.** 1982. Pleiotropic control of five eucaryotic genes by multiple regulatory elements. J. Bacteriol. **151**:1237–1246.
22. **Wickerham, L. J.** 1946. A critical evaluation of the nitrogen assimilation tests commonly used in the classification of yeasts. J. Bacteriol. **52**:293–301.
23. **Zaret, K. S., and F. Sherman.** 1982. DNA sequence required for efficient transcription termination in yeast. Cell **28**:563–573.
24. **Zehner, Z. E., and B. M. Patterson.** 1983. Characterization of the chicken vimentin gene: single copy gene producing multiple mRNAs. Proc. Natl. Acad. Sci. U.S.A. **80**:911–915.